

Atmospheric and oceanic conditions associated with early and late onset for eastern Africa short rains

Article

Published Version

Creative Commons: Attribution-Noncommercial 4.0

open access

Gudoshava, M., Wainwright, C. ORCID: <https://orcid.org/0000-0002-7311-7846>, Hiron, L. ORCID: <https://orcid.org/0000-0002-1189-7576>, Endris, H. S., Segele, Z. T., Woolnough, S. ORCID: <https://orcid.org/0000-0003-0500-8514>, Atheru, Z. and Artan, G. (2022) Atmospheric and oceanic conditions associated with early and late onset for eastern Africa short rains. *International Journal of Climatology*, 42 (12). pp. 6562-6578. ISSN 0899-8418 doi: 10.1002/joc.7627 Available at <https://centaur.reading.ac.uk/104160/>

It is advisable to refer to the publisher's version if you intend to cite from the work. See [Guidance on citing](#).

To link to this article DOI: <http://dx.doi.org/10.1002/joc.7627>

Publisher: John Wiley & Sons

All outputs in CentAUR are protected by Intellectual Property Rights law, including copyright law. Copyright and IPR is retained by the creators or other copyright holders. Terms and conditions for use of this material are defined in the [End User Agreement](#).

www.reading.ac.uk/centaur


CentAUR

Central Archive at the University of Reading

Reading's research outputs online

RESEARCH ARTICLE

Atmospheric and oceanic conditions associated with early and late onset for Eastern Africa short rains

Masilin Gudoshava¹  | Caroline Wainwright^{2,3} | Linda Hirons³ |
Hussen S. Endris¹ | Zewdu T. Segele¹ | Steve Woolnough³ | Zachary Atheru¹ |
Guleid Artan¹

¹IGAD Climate Prediction and Applications Centre (ICPAC), Nairobi, Kenya

²Department of Meteorology, University of Reading, Reading, UK

³National Centre for Atmospheric Science, University of Reading, Reading, UK

Correspondence

Masilin Gudoshava, IGAD Climate Prediction and Applications Centre (ICPAC), Nairobi, Kenya.
Email: masilinstar@gmail.com

Funding information

GCRF African SWIFT, Grant/Award Number: NE/P021077/1; NCAS Atmospheric hazard in developing Countries: Risk assessment and Early Warning

Abstract

Timing of the rainy season is essential for a number of climate sensitive sectors over Eastern Africa. This is particularly true for the agricultural sector, where most activities depend on both the spatial and temporal distribution of rainfall throughout the season. Using a combination of observational and reanalysis datasets, the present study investigates the atmospheric and oceanic conditions associated with early and late onset for Eastern Africa short rains season (October–December). Our results indicate enhanced rainfall in October and November during years with early onset and rainfall deficit in years with late onset for the same months. Early onset years are found to be associated with warmer sea surface temperatures (SSTs) in the western Indian Ocean, and an enhanced moisture flux and anomalous low-level flow into Eastern Africa from as early as the first dekad of September. The late onset years are characterized by cooler SSTs in the western Indian Ocean, anomalous westerly moisture flux and zonal flow limiting moisture supply to the region. The variability in onset date is separated into the interannual and decadal components, and the links with SSTs and low-level circulation over the Indian Ocean basin are examined separately for both timescales. Significant correlations are found between the interannual variability of the onset and the Indian Ocean dipole mode index. On decadal timescales the onset is shown to be partly driven by the variability of the SSTs over the Indian Ocean. Understanding the influence of these potentially predictable SST and moisture patterns on onset variability has huge potential to improve forecasts of the East African short rains. Improved prediction of the variability of the rainy season onset has huge implications for improving key strategic decisions and preparedness action in many sectors, including agriculture.

KEYWORDS

atmospheric drivers, decadal, interannual, oceanic drivers, onset variability

1 | INTRODUCTION

The livelihoods, food security and gross domestic product for most countries in Sub-Saharan Africa are highly dependent on rainfall variability (Barrios *et al.*, 2010; Damania *et al.*, 2020). The climate-sensitive sectors that contribute to these socio-economic factors include the agricultural sector, tourism, water and transport, with agriculture being found to be the key pathway. Approximately 95% of agricultural land use over Sub-Saharan Africa is rainfed (Singh *et al.*, 2011); thus, the sector is heavily dependent on the interannual rainfall variability (Sultan *et al.*, 2020). Eastern Africa is no exception with agriculture playing a critical role in enhancing food security and improving livelihoods over the region. Consequently, reliable and actionable forecast information on the intra-seasonal variability of rainfall has the potential to better support decision-making in the agricultural sector. For instance, knowledge on the beginning of the rainy season (onset of the rainfall) is key for making strategic decisions (Owusu *et al.*, 2017) such as time of planting, the crop varieties and choice of crop to plant. If farmers anticipate a later onset there is a likelihood that they will not prepare the land on time which, if the rains come early, will likely affect the growing period of the crops. Likewise, if a crop is planted too early there is a likelihood that it will wilt before reaching maturity. Thus, unexpected onset variability is clearly linked to increasing food insecurity.

Eastern Africa straddles the equator; thus, it is directly impacted by seasonal changes in the Hadley circulation. The region is characterized by three major rainfall seasons, the March–May (MAM), June–September (JJAS) and the October–December (OND). These rainy seasons accompany the meridional shift of the inter-tropical convergence zone (ITCZ), moving from the southern to the northern hemisphere during the MAM and JJAS season and back to the southern hemisphere during the OND season (Asnani, 1993; Nicholson, 2017). The equatorial region is characterized by a bimodal rainfall distribution, that is the MAM (commonly known as the long rains) and the OND (known as the short rains) seasons. In this study we focus on the October–December season. The season is important for the numerous climate sensitive sectors over the region and accounts for more than 60% of total annual rainfall over eastern parts of Kenya (Figure 1). In October the rainfall is mostly confined over the northern parts and equatorial sector of the region (Figure S1, Supporting Information). As the season progresses, the rainfall band moves southwards, with rainfall mostly confined to the equatorial region in November. In December most of the rainfall is received over Tanzania with the northern and equatorial regions generally dry.

Several studies over the region have focused on the interannual variability of seasonal rainfall (e.g., Ogallo, 1988; Beltrando, 1990; Anyah and Semazzi, 2007; Ongoma and Chen, 2017). For example, a relationship between the short rains and El Niño–Southern Oscillation (ENSO) has been demonstrated in several studies (e.g., Ogallo, 1988; Nicholson and Kim, 1997; Mutai *et al.*, 1998; Indeje *et al.*, 2000). It was shown that enhanced rainfall is associated with warming sea surface temperatures (SSTs) over the Pacific Ocean. The SST patterns and zonal winds over the Indian Ocean were also shown to be strongly related to the short rains precipitation in Eastern Africa (e.g., Beltrando and Camberlin, 1993; Ogallo and Janowiak, 1988; Black *et al.*, 2003; Black, 2005; Ummenhofer *et al.*, 2009; Hirons and Turner, 2018). The Indian Ocean Dipole (IOD) describes the opposite SST anomalies in the eastern and western tropical Indian Ocean. Positive IOD events, with warm SST anomalies in the western Indian Ocean and cool SST anomalies in the eastern Indian Ocean, have been linked to enhanced rainfall over Eastern Africa, while negative IOD events are linked to suppressed rainfall during the short rains season. The location of the eastern ridge of the Mascarene High was also found to be linked to the interannual variations of the short rains (Manatsa *et al.*, 2014; Hirons and Turner, 2018). When the Mascarene High eastern ridge shifts to the west the region experiences suppressed rainfall.

OND contribution to Annual Rainfall

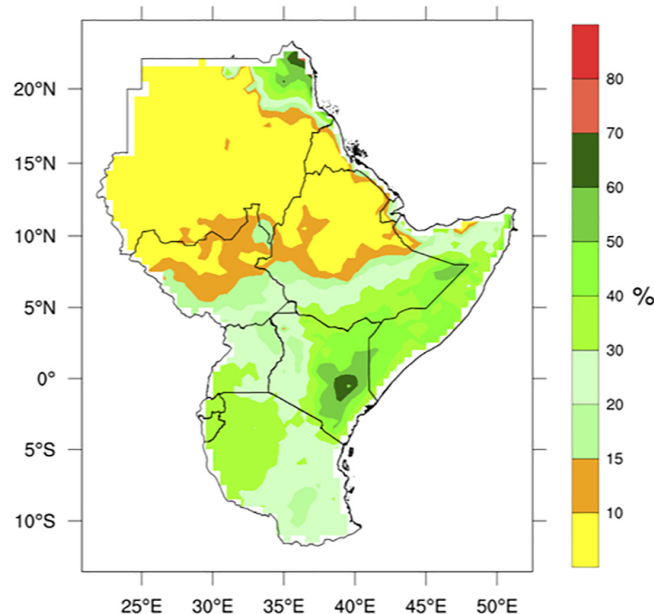


FIGURE 1 Percentage contribution of the short rains season to total annual rainfall over Eastern Africa

In addition to the interannual variability numerous studies over Eastern Africa have investigated the decadal variability of rainfall (e.g., Nicholson, 2000; Schreck III and Semazzi, 2004; Omondi *et al.*, 2012; 2013; Tierney *et al.*, 2013). During the short rains some regions over Eastern Africa have been shown to experience strong decadal signals (Schreck III and Semazzi, 2004). Omondi *et al.* (2012) investigated the modes of decadal rainfall variability over Eastern Africa and their predictability potentials using global SSTs. The study showed that the MAM and OND seasons are dominated by 10-year cycles of wet and dry phases, while the June–August season showed 20-year cycles of wet and dry phases. Tierney *et al.* (2013) showed that on multidecadal timescales, the Indian Ocean drives Eastern African rainfall variability by altering the local Walker circulation, whereas the influence of the Pacific Ocean is minimal. Despite the scientific advancement in understanding the interannual and decadal rainfall patterns over Eastern Africa, a limited number of studies have focused on the rainfall onset, yet the timing of onset is crucial for humanitarian resource mobilization, agriculture and reservoir management. Hence, having improved knowledge on the variability of rainfall onset has the potential to build more resilient livelihoods and communities.

Camberlin and Okoola (2003) investigated the relationship between onset and large-scale atmospheric and oceanic fields during the Eastern Africa MAM season on a monthly timescale. The study found that the interannual variations in the MAM season onset are linked to SSTs and sea-level pressure patterns that have a different sign over the Atlantic and Indian Oceans. A warm South Atlantic and a cool Indian Ocean are associated with low and high sea level pressure anomalies, respectively, that lead to late onset over the region. The study also found a relationship between the onset of rainfall over Eastern Africa and equatorial zonal winds (zonal wind averaged over 20°–35°E, 5°S–5°N). Anomalous equatorial easterlies and surface divergence over Eastern Africa maintain the meridional branch of the ITCZ further west resulting in late onset over the region during the MAM season. MacLeod (2018) investigated the role of zonal wind index found in Camberlin and Okoola (2003) on the onset of the MAM and OND seasons over Eastern Africa. The study found that there was a weak link between the zonal wind index and onset over the region during the OND season. Wainwright *et al.* (2019) found that the meridional SST gradient over the Indian Ocean has a teleconnection with the rainfall onset over Eastern Africa during the MAM season. Warmer SST south of Madagascar generally leads to late onset by delaying the northward progression of the rain-band. Okoola (1999) suggested that at the onset of the MAM season, easterlies

are dominant near the equator and westerlies near 15°S in the lower troposphere. Kijazi and Reason (2005) studied the link between ENSO and rainfall onset over coastal Tanzania. The study found that the increased OND seasonal rainfall during El Niño events is associated with an early onset. Focusing on the Eastern Africa region, Dunning *et al.* (2016) demonstrated that ENSO events had minimum impact on the onset of the short rains. Evidently the scientific analysis on rainfall onset has mostly focused on the long rains season with only a few studies conducted to understand the possible drivers during the short rains season, an equally important season for agricultural activities over the region. Thus, there remains a gap in the understanding of what drives onset variability during the short rains season.

In this study we investigate the atmospheric and ocean conditions prior to and during the onset of the short rains season over Eastern Africa. It is crucial to know the atmospheric conditions before, during and immediately after the rainfall onset in order to improve the prediction of onset. Improved understanding of drivers has the potential to improve forecasts of onset at longer lead times provided the drivers and local response can be adequately represented in models. This has implications for improved action-based forecasting in the various climate-sensitive sectors.

2 | DATA AND METHODS

2.1 | Data

Daily rainfall data for onset calculation was obtained from the Climate Hazard Infrared precipitation with stations (CHIRPSv2; Funk *et al.*, 2015). The data are available from 1981 to near present and has a high spatial resolution of 0.05°. We choose this dataset as it has a high temporal and spatial resolution; in addition, it is available over a longer time period in comparison with other daily satellite datasets. The dataset has been evaluated over Eastern Africa by a number of studies including Kimani *et al.* (2017), Dinku *et al.* (2018) and Ayugi *et al.* (2019). These studies have shown that the dataset is able to reproduce the rainfall total and variability over the region though skill is lower over mountainous regions.

The European Centre for Medium-Range Weather Forecasts (ECMWF) fifth generation reanalysis (ERA5; Hersbach *et al.*, 2020) datasets were used in characterizing the atmospheric conditions before, during and immediately after the onset of the Eastern Africa Short Rains. The global dataset is available from 1979 to near present with a 0.25 resolution. In this study hourly low-level zonal, meridional winds and vertically integrated

eastward and northward water vapour fluxes from 1981 to 2019 are combined to form the dekadal (10 day) averages. The vertically integrated eastward and northward water vapour fluxes are derived quantities and are pre-calculated by the ECMWF.

Sea surface temperatures are obtained from the Optimum Interpolation Sea Surface Temperature (OISST v2.1) analysis. The datasets are available from 1981 to near present at a resolution of 0.25° . The dataset is constructed by combining observations from different platforms such as satellites, ships, buoys, and Argo floats on a regular global grid (Reynolds, 1993; Banzon *et al.*, 2020).

2.2 | Methods

2.2.1 | Onset algorithm

Various techniques are utilized in the calculation of rainfall onset; these include those that solely utilize rainfall and those that utilize various meteorological variables. Methods that solely use rainfall include those that utilize threshold values on accumulated rainfall (also known as agro-climatic definition, e.g., Sivakumar, 1988; Marteau *et al.*, 2009; 2011; Recha *et al.*, 2012; Philippon *et al.*, 2015), percentage cut-off on accumulated rainfall (Odekunle, 2004) and the sum of accumulated anomalies (Marengo *et al.*, 2001; Dunning *et al.*, 2016). Agro-climatic based onsets are defined based on crop water satisfaction above a predefined threshold value for a particular crop (e.g., Sivakumar, 1988; Marteau *et al.*, 2009; Philippon *et al.*, 2015). To avoid detection of a false onset an additional criterion stipulates that the region is not supposed to have continuous dry days of a certain number of days in the following stipulated days after onset has been detected (e.g., Sivakumar, 1988; Segele and Lamb, 2005; Recha *et al.*, 2012).

In this study, we adopt the agro-meteorological definition of onset, which is currently being utilized operationally over Eastern Africa. Onset is defined as the first day of the wet season when a wet spell of accumulated rainfall in three consecutive days is at least 20 mm and there is no dry spell of at least 7 days in the next 20 days. The threshold for a rainy day is defined as 1 mm. This definition has previously been applied over the region (e.g., Segele and Lamb, 2005; Gudoshava *et al.*, 2020). The onset is calculated from 15 days before the anticipated start of the season. In this case the start date was 15 September. It must be noted that the shortcomings of a single threshold value for onset are that the threshold can be too high for some regions, for example over the arid and semi-arid lands (ASALs). However, at regional level we utilize the same threshold and encourage use of different thresholds at the national level. An example of using different thresholds

can be found in Segele and Lamb (2005). Onset dates are calculated over a 39-year period (1981–2019). The standardized anomalies for the onset were obtained by first removing the mean, then dividing the anomalies by the climatological standard deviation and averaging over the region that receives at least 15% of the annual total rainfall (Figure 1). To ensure robustness of the results sensitivity analysis is performed utilizing two other rainfall masking thresholds (20 and 30%). Using each of these timeseries composite analysis is then conducted.

2.2.2 | Dynamical drivers characterization

Composite analysis using the standardized onset anomalies on the various meteorological variables was conducted to obtain the atmospheric conditions for early, normal and late onset. The early, normal and late onset thresholds used in composite analysis are described further in section 3.1. Composite analysis has been extensively used over the Greater Horn of Africa to characterize the state of the global climate drivers for seasons with enhanced and depressed rainfall (Okoola, 1999; Indeje *et al.*, 2000). This study utilizes dekadal time periods for the months of September and October to construct the composites for the various atmospheric fields and SST.

2.2.3 | Interannual and decadal variability

We further explore the influence of interannual and decadal (10 year) variability separately on onset variability over the region. Different techniques have been utilized over the region for signal processing including wavelet analysis, binomial filter (e.g., Omondi *et al.*, 2012), Butterworth filter (e.g., Bahaga *et al.*, 2019) and the Fast Fourier decomposition (e.g., Awange *et al.*, 2008). In this study timeseries decomposition for low- and high-frequency modulation is done utilizing the Fast Fourier decomposition. We choose a wave number of 1–5 for low-frequency modulation (corresponding to periods ≥ 7.8 years) and 6–19 for the high-frequency modulation (corresponding to periods ≤ 6.5 years). The high frequency will be used to analyse the interannual variability, while the low frequency will be used for the decadal variability. Filtering is done on the onset dates, and the atmospheric and oceanic drivers (winds and SSTs).

2.2.4 | The dipole mode index

The Indian Ocean Dipole (IOD) is a coupled ocean and atmosphere phenomenon that plays a critical role in

modulating the Eastern Africa short rains (e.g., Black *et al.*, 2003; Ummenhofer *et al.*, 2009; Hirons and Turner, 2018). As an indicator of the IOD, the dipole mode index (DMI) is defined by calculating the SST

gradient between the western Indian Ocean (10°S – 10°N , 50° – 70°E) and the southeastern Indian Ocean (10°S – 0°N , 90° – 110°E ; Saji *et al.*, 1999). The index is also filtered for the interannual analysis.

3 | RESULTS AND DISCUSSION

3.1 | Mean rainfall onset

The standardized anomalies for onset of the short rains, spatially averaged over the region that receives above 15% of annual rainfall during the OND season (Figure 1) are shown in Figure 2. Over the region early onset mostly occurs during 1981–1990 and 2011–2019, while late onset mostly occurs during 1991–2010. The timeseries of onsets shows both high-frequency interannual variability and a low-frequency modulation of the onset (Figure 2). Further discussion of the high- and low-frequency modulation is found in section 3.6. In the initial (unfiltered) analysis we use the years marked with red squares for early onset composites (standardized anomalies less than -0.2) and the blue circles for the late onset composites (standardized anomalies greater than 0.2). Nine years are identified as early onset using a threshold of -0.2 and 13 years are identified as late onset years. The normal onset is calculated using the years not marked by either

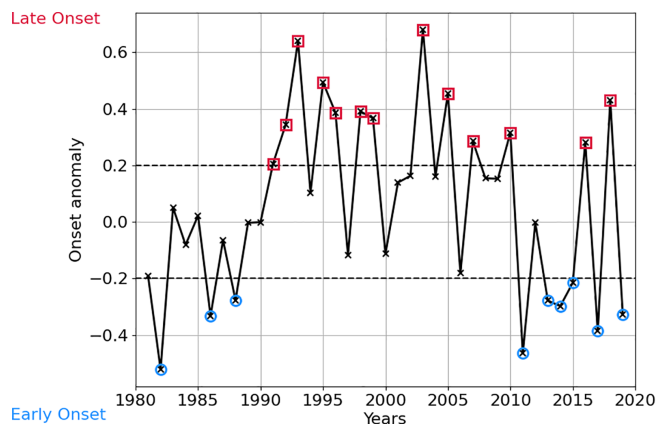


FIGURE 2 Standardized onset anomalies time series for Eastern Africa short rains utilizing the CHIRPS daily datasets (1981–2019). The entire timeseries was utilized in computing the standardized anomalies. The dashed black horizontal lines represent the thresholds utilized for the early onset (≤ -0.2) and late onset (≥ 0.2). The blue circles represent the identified early onset and the red squares represent late onset years

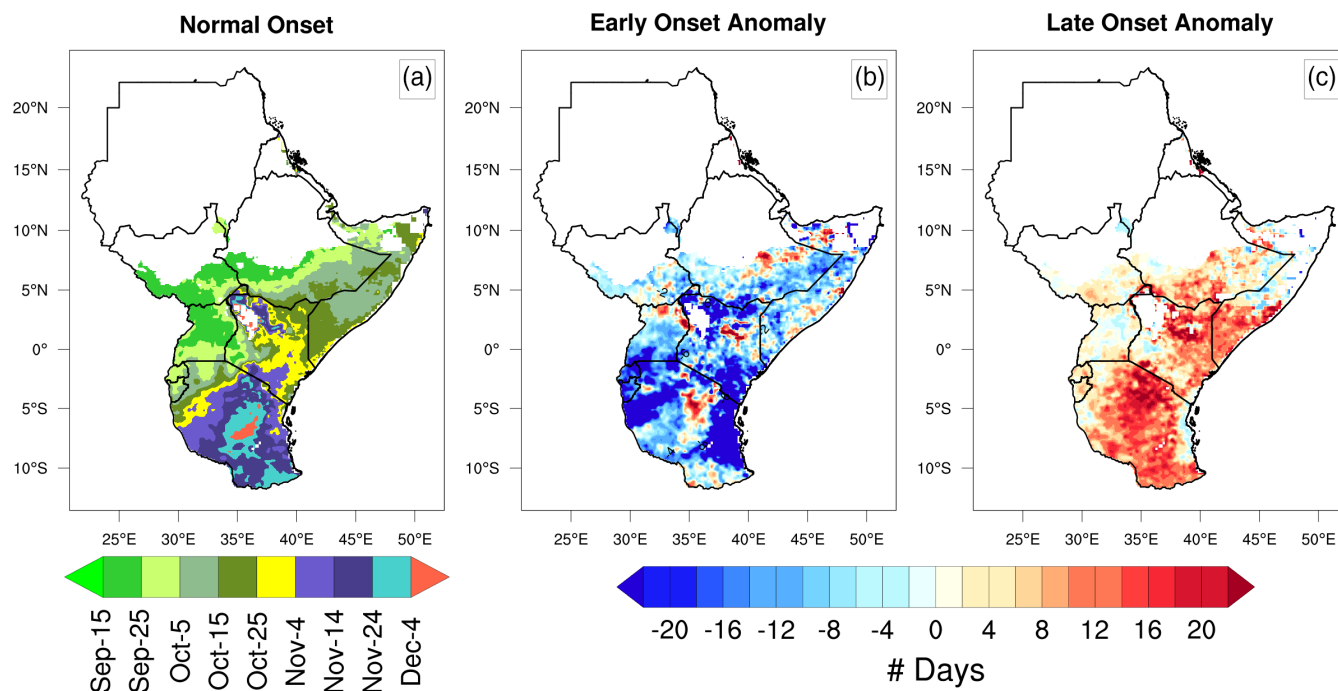


FIGURE 3 Onset date and anomaly for Eastern Africa short rains utilizing the CHIRPS daily datasets. (a) Normal onset dates (average of the years with standardized anomalies between -0.2 and 0.2), (b) early onset anomaly (composite of years with standardized anomalies ≤ -0.2), (c) late onset anomaly (composite of years with standardized anomalies ≥ 0.2)

the red squares or blue circles. All anomalies for unfiltered data will be calculated relative to these years. We proceed to analyse the spatial variation of onset.

The Eastern Africa short rains onset commences from the northern parts of the region, over southern parts of Ethiopia and South Sudan in September and advances southwards to Tanzania by late November consistent with the boreal autumn southward movement of the inter-tropical convergence zone (Figure 3a). This north–south pattern is consistent with other studies over the region (Camberlin *et al.*, 2009; Dunning *et al.*, 2016; MacLeod, 2018). Using the early and late onset years shown in Figure 2, Figure 3b,c show the early and late onset anomalies respectively over the region. Anomalies are calculated relative to the normal onset years shown in Figure 3a. Overall, during early/late onset years the majority of the region displays a consistent early/late onset signal, with only a few localized areas that are not consistent with onset anomaly over the region. The localized areas are mostly the transitional regions, which experience rainfall during the June–September season. The spatial coherence in the onset anomalies is consistent with what has been shown previously for total rainfall over the region (Ogallo, 1989; Beltrando, 1990). Early onset occurs up to more than 20 days earlier compared to the normal onset over parts of Tanzania, Kenya and Uganda while the late onset is delayed by approximately more than 20 days over parts of Tanzania (Figure 3c).

Normal onset dates exhibit high temporal variability over Tanzania, Kenya and southern parts of Ethiopia

(Figure 4), and least variable over parts of Ethiopia, Uganda, South Sudan and Somalia. The standard deviation in the normal onset is approximately 20 days over parts of Tanzania, about 12 days over parts of Kenya and Ethiopia and up to 8 days over parts of Uganda, South Sudan and Somalia. For early onset the variability of onset dates is approximately 8 days over the northern parts of the region and in Uganda and up to 20 days over the southern parts of the domain. For late onset variability is also over 20 days over the southern parts of the region. The large interannual variability during the short rains has been report before for total rainfall (e.g., Ogallo, 1989) and for the rainfall onset (Camberlin *et al.*, 2009). However the standard deviations found in this study are slightly lower than those obtained in Camberlin *et al.* (2009) of approximately 24.7 over Kenya and Tanzania. The difference could be due to the time period analysed; in addition, in this study we separated the normal, early and late onset years. The standard deviation results indicate that in regions that receive rainfall during the boreal summer the onset variability is lower relative to areas that were dry in the previous season.

3.2 | Rainfall in early and late onset years

To study the relationship between onset and monthly total rainfall, composite analysis is conducted. In October most of the rainfall is concentrated in the northern and

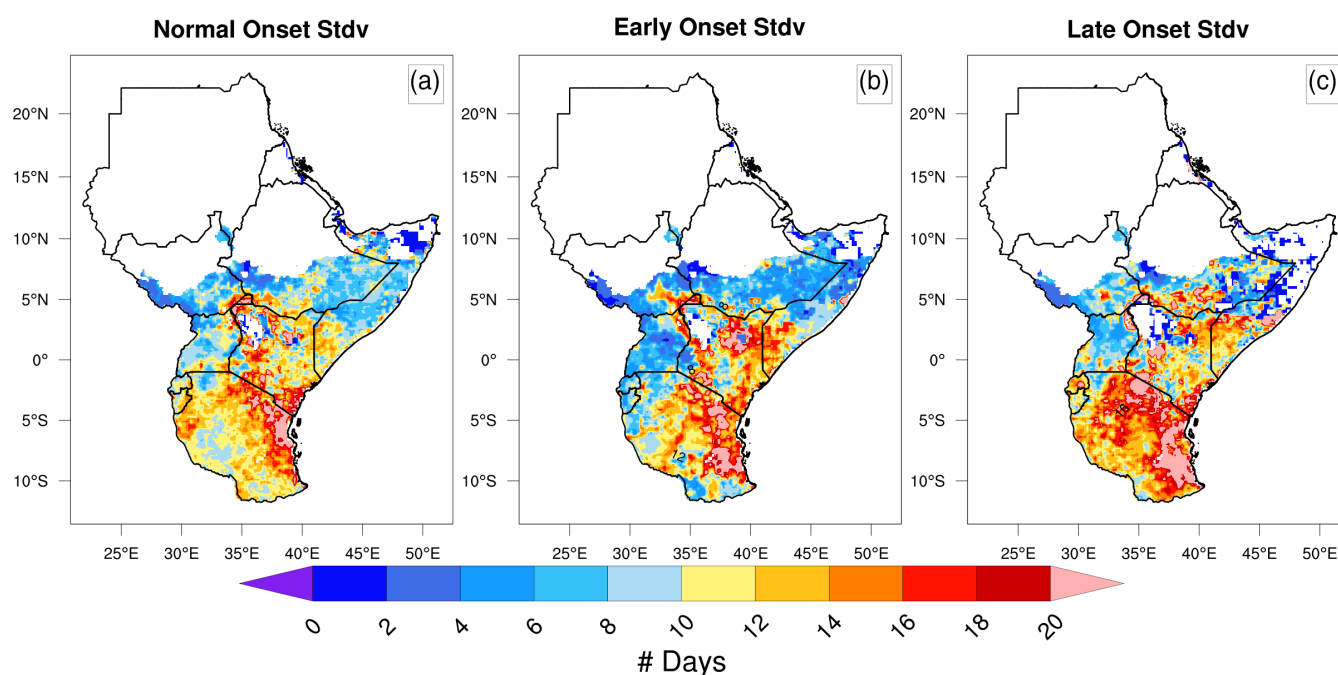


FIGURE 4 Standard deviation of the onset dates for Eastern Africa short rains utilizing the CHIRPS daily datasets. (a) Normal onset spread, (b) early onset spread, (c) late onset spread

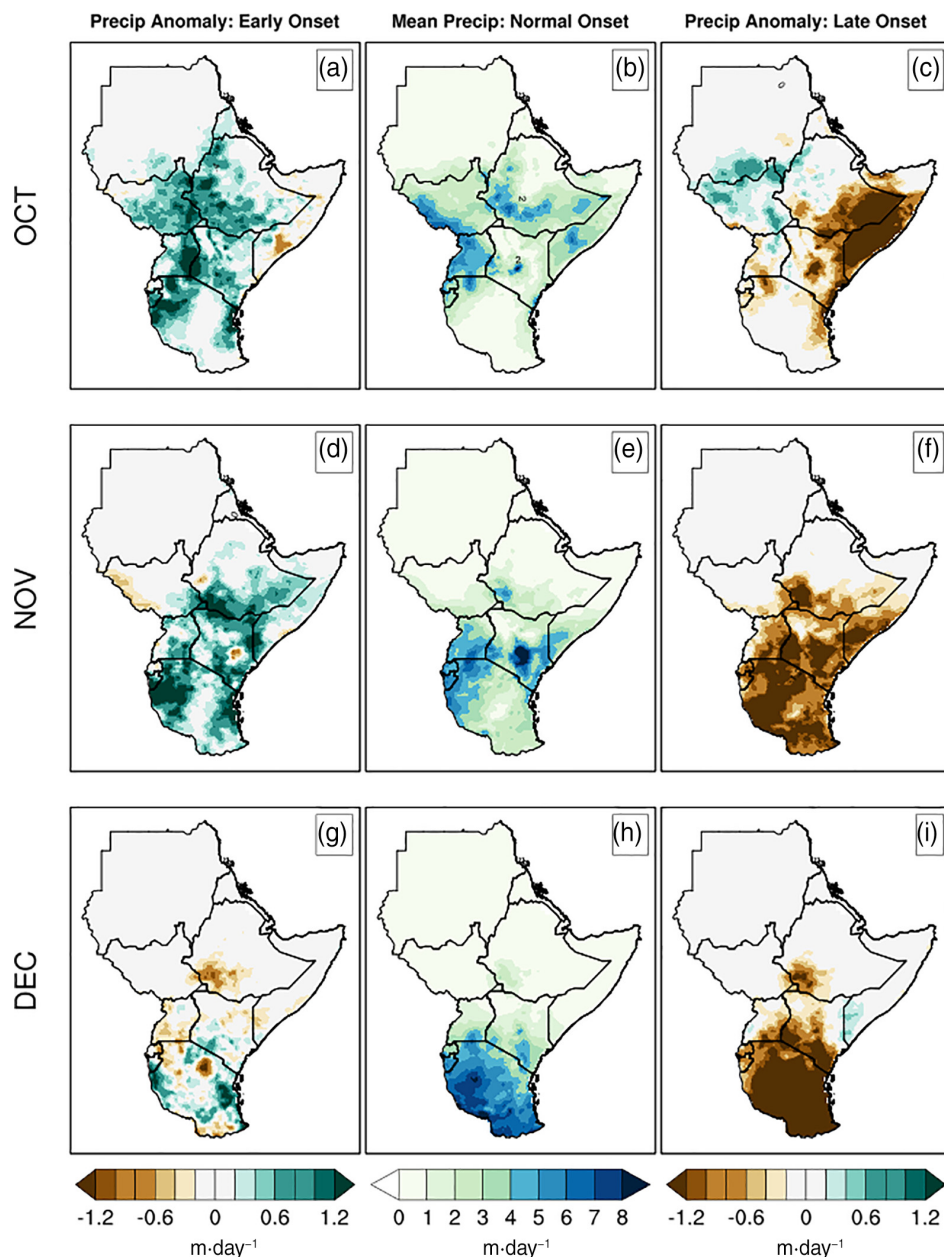


FIGURE 5 Mean daily rainfall composites for early onset anomaly (left column), daily mean rainfall (middle column) and a late onset anomaly (right) during the short rains for each month (October–December) over Eastern Africa

equatorial region of Eastern Africa (Figure 5b). During this time the southern parts of the region are generally dry. Early onset is associated with enhanced rainfall over the equatorial and northern parts of the region during the month of October (Figure 5a), while late onset is associated with a rainfall deficit that is concentrated over parts of eastern and coastal Eastern Africa, specifically over parts of Somalia, southeast Ethiopia, central Kenya and coastal parts of Kenya and Tanzania (Figure 5c). In addition, during the late onset years in October northern South Sudan and southern Sudan are wetter than usual indicating the rain band is further north. In November, the peak of the short rains season, rainfall is concentrated mostly over the equatorial and southern parts of Eastern Africa (Figure 5e). During November early onset is

associated with enhanced rainfall over most parts of the region, whereas the late onset is associated with a rainfall deficit. In December, which is normally the short rains cessation, parts of the equatorial region and most of the southern region receive rainfall while the other parts are dry (Figure 5h). In December the early onset years have relatively weak wet anomalies, possibly indicating that early onset is not associated with heavy rainfall towards the end of the season (Figure 5g). However for late onset, the total rainfall is strongly reduced in the month of December over parts of Tanzania (Figure 5i). It must be noted that most parts of Tanzania have a unimodal rainfall season, with the onset in late November and cessation at the beginning of April. In addition to showing the normal onset mean precipitation we also conducted

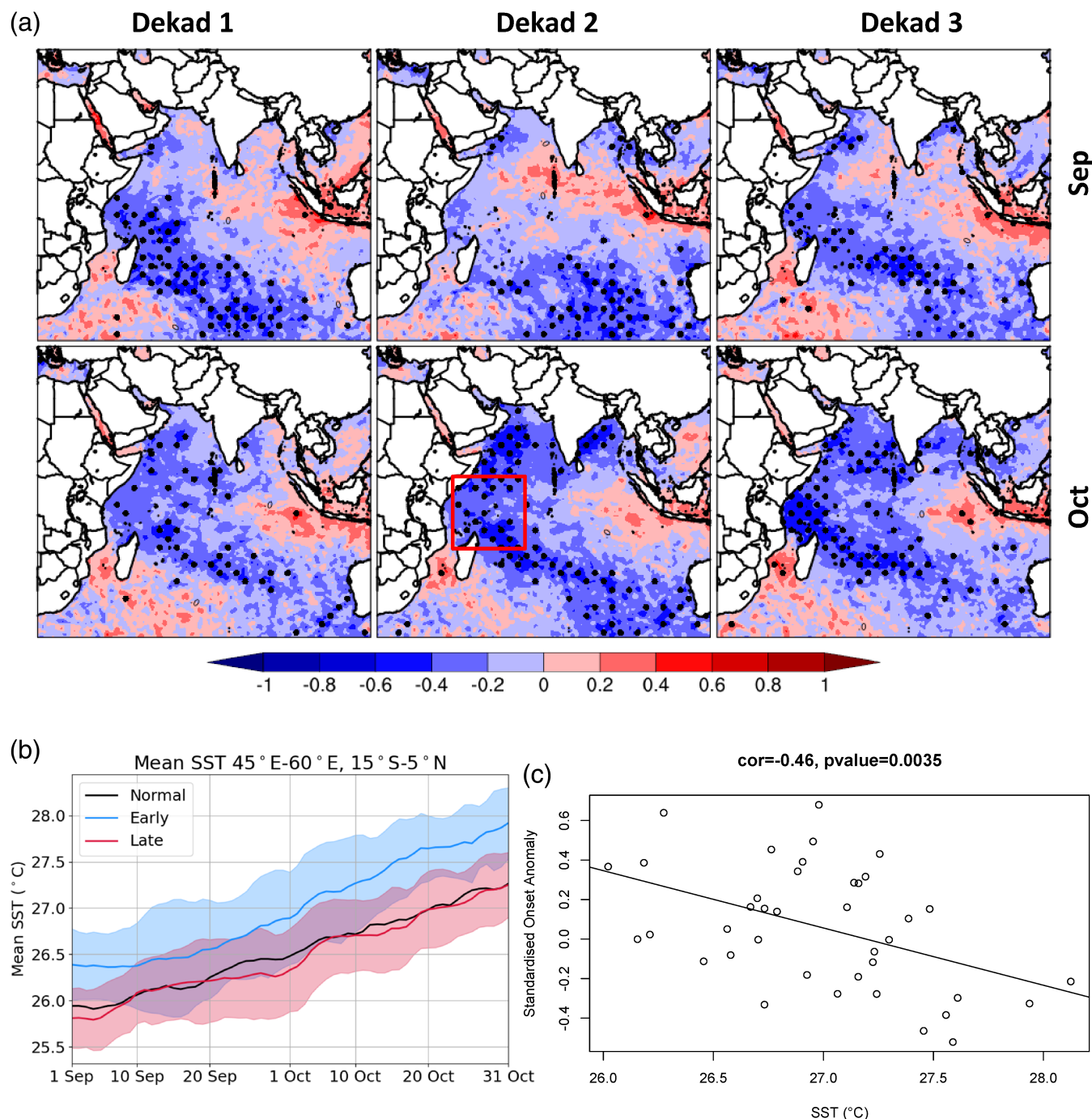


FIGURE 6 Correlation of the SST and the short rains onset anomaly from CHIRPS from 1981 to 2019. (a) Onset anomaly correlation and the SST for each grid point over the Indian Ocean Basin. The black dots represent correlations that are statistically significant at the 5% significance level. (b) Evolution of the SST over western Indian Ocean (45° – 60° E and 15° S– 5° N). The shading in the plot represents the standard deviations of the SST. (c) Relationship of SST and onset anomaly utilizing the box 45° – 60° E and 15° S– 5° N for the second dekad of October

composite analysis for the anomalies during the mean onset years. During the normal onset years rainfall anomalies are very small and close to zero except over parts of Somalia that has positive anomalies however the anomalies are smaller in comparison to those in early onset years. In December the anomalies are mostly positive over Tanzania, but, still smaller in comparison to the early onset years (Figure S2).

3.3 | Role of sea surface temperature

Numerous studies have shown the important role that the SSTs over the Indian Ocean basin exert on the total rainfall during the short rains (Behera *et al.*, 2005; Ummenhofer *et al.*, 2009; Liu *et al.*, 2020). Hence, in this study we explore the role of the Indian Ocean SST on the onset variability. The Indian Ocean is chosen, as this is

the major source of the moisture into the Eastern Africa region during the short rains. Interannual correlations between onset and SST are computed using the Pearson correlation for six dekads from September to October (Figure 6). The rainfall onset is negatively correlated (correlation less than -0.4) with the SSTs over the western Indian Ocean; this indicates that early onset is associated with warm SSTs over the western Indian Ocean. The region of negative SST correlations stretches diagonally from the coast of East Africa to the region of the semi-permanent Mascarene high-pressure system (Figure 6a). A positive correlation between total rainfall and SST has been seen in previous studies in the same region (Black, 2005; Ummenhofer *et al.*, 2009; Liu *et al.*, 2020), consistent with a link between early onset and increased seasonal rainfall. Statistically significant correlations are evident from dekad one of September (1st–10th September); however, the correlations reduce in the second dekad of September, and thereafter the correlations gradually increase to dekad 3 of October (Figure 6a). Dekad 2 and dekad 3 of October have the largest spatial extent of statistically significant correlation coefficients. The evolution of the SSTs over time for the region 45° – 60° E and 15° S– 5° N (red box; Figure 6a) over western Indian Ocean indicates that SST gradually increases from September to October (Figure 6b). During the early onset years the SSTs over western Indian Ocean basin (red box; Figure 6a) are warmer; however, there is no clear distinction of the SST for the late and normal onset years (Figure 6b). Late onset is associated with cooler SST, while early onset is associated with warmer SSTs (Figure 6c). Utilizing the 20 and 30% masking threshold it is shown that the relationship between the onset timeseries and the SST remains the same (Figure S3). The correlations between the onset timeseries and the SST for the 20% threshold are highest in dekad 2 of October and lowest in dekad 2 of September, consistent with the results for the 15% masking. A 30% rainfall masking threshold also shows similar results with the 15 and 20% thresholds though with higher correlations between the SSTs over western Indian Ocean and onset timeseries.

3.4 | Sea surface temperatures and vertically integrated moisture flux

Composite analysis for the rainfall onset and the SST is conducted to investigate the mean state of the Indian Ocean during the early, normal and late onset years. During the early onset years the SSTs over the Indian Ocean are generally warmer compared to the SSTs associated with normal onset (Figure 7). The warming anomaly

slightly reduces in September dekad 2 and 3; thereafter, the warming anomaly gradually increases consistent with the correlation patterns in Figure 6. The SST anomaly for the late onset years is mostly negative; however, the values are close to zero, implying that the cooler signal for late onset is weak. These results show that early onset is linked to the warming of the SSTs over the Indian Ocean, but indicates that there is no distinct difference between the normal and late onset years consistent with Figure 6b. The SST anomalies during the normal onset years are also computed and are small (not shown).

We further investigate the composites of vertically integrated moisture fluxes with early and late onset years. While no discernible differences are evident from the composite analysis of the vertically integrated moisture fluxes in September, differences exist for early and late onset in October. In early onset years there is an anomalous equatorial easterly moisture advection into Eastern Africa during the first two dekads of October (Figure 7). The enhanced moisture flux is due to the warm SST anomalies in the western Indian Ocean that result in increased atmospheric moisture content and enhanced local convective activity, hence early onset. During the late years anomalous westerly flow is dominant and limits moisture into the region. This pattern weakens in dekad 3 of October, possibly indicating other mechanisms dominate towards the peak of the rainy season.

3.5 | Low-level circulation

MacLeod (2018) investigated the role of the 700-hPa low-level zonal winds on the onset of the short rains. The study focused on a monthly timescale and found a weak link between the rainfall onset and zonal winds. In this study we investigate the link between the short rains onset and zonal winds at a lower pressure level and dekadal timescales. 850 hPa is chosen as this is the pressure level that is used to characterize the Somali low-level jet (Boos and Emanuel, 2009); an important source of moisture over the region (Riddle and Cook, 2008). Figure 8 shows the low-level (850 hPa) circulation (vectors) and mean zonal flow (shaded) for the early, normal and late onset years for September and October. The mean flow is dominated by the southeasterly flow in the southern equatorial region and northwesterly flow in the northern equatorial region. Mean southeasterly and northwesterly flows during the normal onset years are stronger during the month of September and weaker during October. In September, from dekad 1 to dekad 3 there are no salient differences in the mean flow for the early and late onset years in the black box highlighted on the

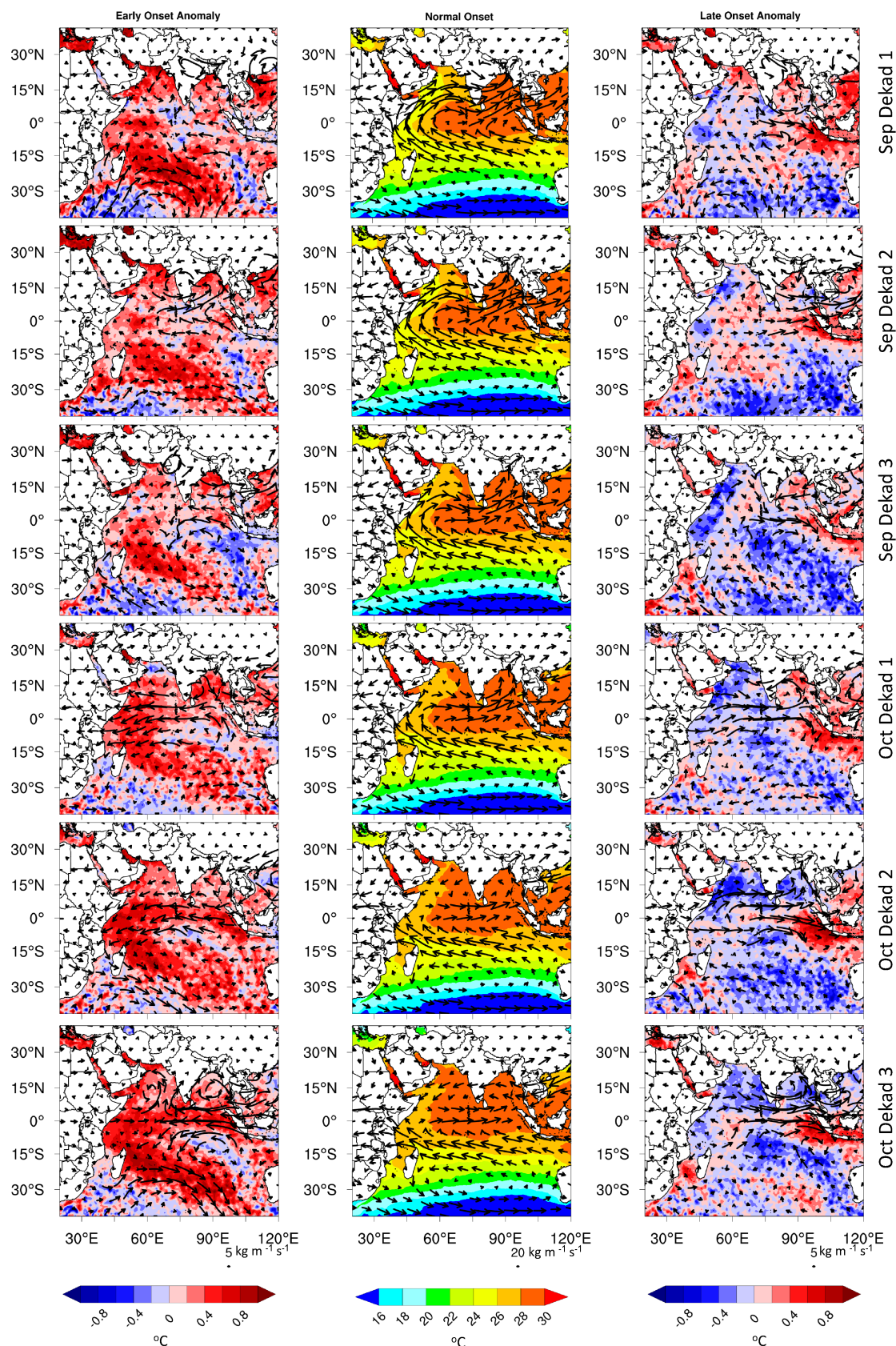


FIGURE 7 Vertically integrated moisture flux (vectors, $\text{kg m}^{-1} \text{s}^{-1}$) and sea surface temperatures (shaded, $^{\circ}\text{C}$) composites for the early onset anomaly (left column), mean onset (middle column) and late onset anomaly (right column) over Eastern Africa, from Dekad 1 of September (top row) to Dekad 3 of October (bottom row)

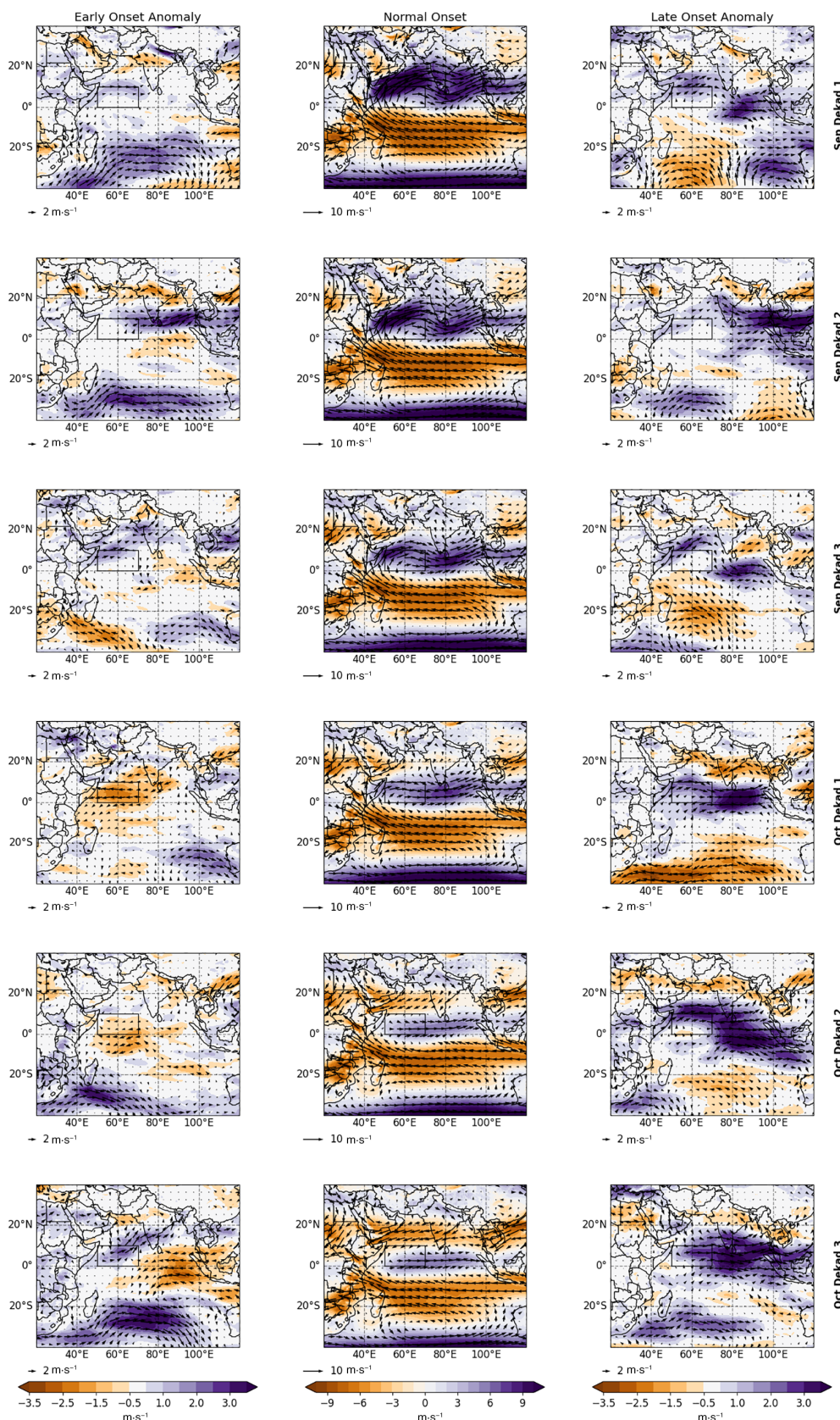


FIGURE 8 Mean flow (vectors) and zonal flow (shaded) composites for the early onset anomaly (left column), normal onset (middle column) and late onset anomaly (right column) over Eastern Africa from September dekad 1 (top row) to October dekad 3 (bottom row)

plots. In dekad 1 of October early onset is linked to anomalous easterlies, while for the late onset years late anomalous westerlies dominate the flow. The flow

weakens in the second and third dekad of October however the pattern observed in dekad 1 of October persists.

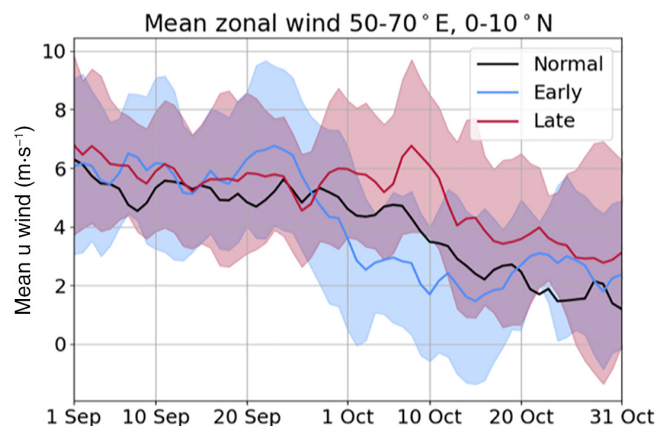


FIGURE 9 Evolution of the zonal wind flow over the region 50° – 70° E, 0° – 10° N for the early (blue), normal (black) and late (red) onset

An analysis of the evolution of the mean zonal winds near the Somali coastal region (50° – 70° E, 0° – 10° N) indicates that there are no notable differences in the mean zonal winds in September; however, in October there are differences in the mean zonal winds (Figure 9). Stronger westerlies dominate the flow in late onset years, while weaker westerlies dominate during early onset years. This consequently implies that more moisture is drawn out of the region during the late onset years, leading to a delay in the start of the rainy season. The separation in the strength of the westerlies reduces in the third dekad of October.

Limited studies have investigated the link between the rainfall onset and the migration of the ITCZ (Camberlin and Okoola, 2003; Kijazi and Reason, 2005; Mugalavai *et al.*, 2008; Dunning *et al.*, 2016; 2018; Wainwright *et al.*, 2019). Sohn and Park (2010) showed that moisture convergence flux intensifies in areas with ascending motions along the ITCZ. Dunning *et al.* (2016) showed that the onset of rainfall over Africa is consistent with the migration of the ITCZ. The intensification of the Saharan Heat Low was found to influence the southward progression of the tropical rain belt (Dunning *et al.*, 2018). It was found that during the boreal summer the rainband travels further north and stays north longer, delaying the southward retreat (Dunning *et al.*, 2018) which could lead to a late onset over Eastern Africa. Camberlin and Okoola (2003) found that the modified pressure gradient between the Atlantic and Indian Ocean basins and enhanced easterlies over land prevent the meridional branch of the ITCZ from expanding to the east over East Africa, hence delaying the rainy season onset during the long rains. In addition to the modified pressure gradient, Wainwright *et al.* (2019) found that warmer SST south of Madagascar delayed the northward

progression of the rainband during the long rains season. We hypothesise that during the early onset years for the short rains, the warm SSTs in the western Indian Ocean, and southwesterly wind anomalies off the coast of Somalia support the southward retreat of the rainband and earlier establishment of rainfall over Eastern Africa. The easterly moisture flux in early onset years also provides moisture to support early onset of the rainfall in such years.

3.6 | Interannual and decadal variability

Since the timeseries for onset shows both interannual and decadal variability we use a Fourier transform to obtain the low- and high-frequency modulation. Figure 10 shows the filtered low-frequency and high-frequency timeseries. The low-frequency timeseries indicates that in the first and last 10 years the region mostly experienced early onset while in the middle 19 years the region experienced late onset (Figure 10a). The high-frequency timeseries shows a relatively uniform distribution of early, normal and late onset years with no obvious time period being dominated by a single category. In order to explore the high-frequency (interannual) component the 10 earliest and 10 latest years of the high-frequency filtered timeseries were selected; the other 19 years that are not marked with either red or blue in Figure 10b comprises the normal onset years. To explore the low-frequency (decadal) variability, the periods from 1981 to 1990 and 2010 to 2019 were compared with the period 1991–2009. Dekad 1 of October is utilized for the interannual and decadal analysis as this is the first dekad with distinct different flow for early and late onset; in addition, the SST over the western Indian Ocean has a relatively high correlation with the rainfall onset.

3.6.1 | Sea surface temperature

We explore the relationship between SSTs over the Indian Ocean basin with the rainfall onset on both decadal and interannual timescales. The mean SST has a gradual decrease from the northern part of the Indian Ocean to the southern part of the basin (Figure 11b). On decadal timescales, in the early onset years the Indian Ocean is warmer (Figure 11a), while for the late onset years the basin is cooler (Figure 11c). The interannual variability analysis shows that for the normal onset anomaly years the western and eastern parts of the Indian Ocean basin are warmer than during the mean onset years while the central part is cooler (Figure 11e). For the early onset years (Figure 11d) the western and

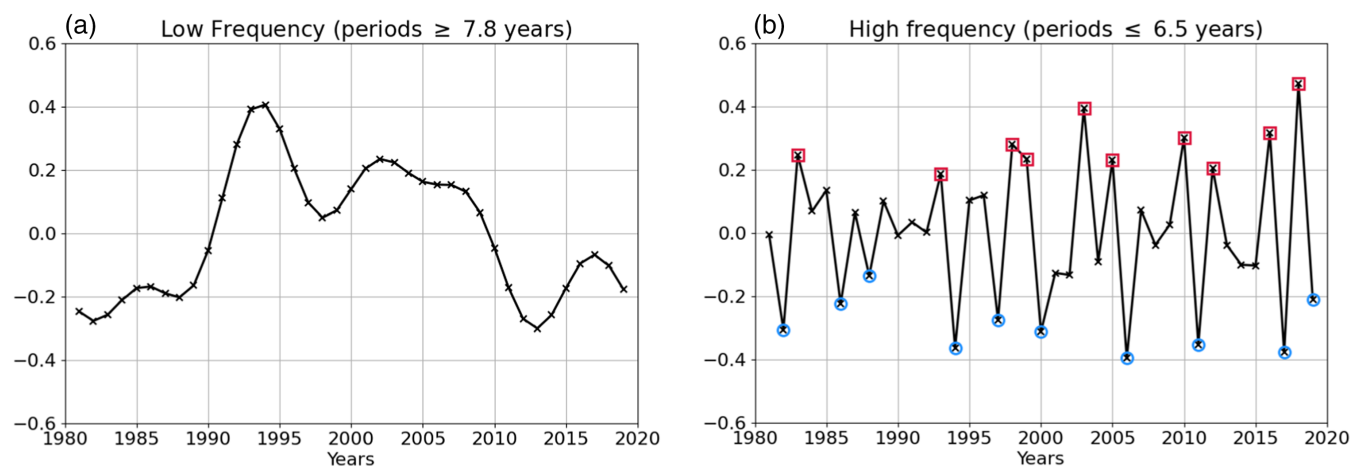


FIGURE 10 Filtered CHIRPS onset timeseries (1981–2019) for (a) low-frequency (≥ 7.8 years) and (b) high-frequency periods (≤ 6.5 years) utilizing the fast Fourier transform

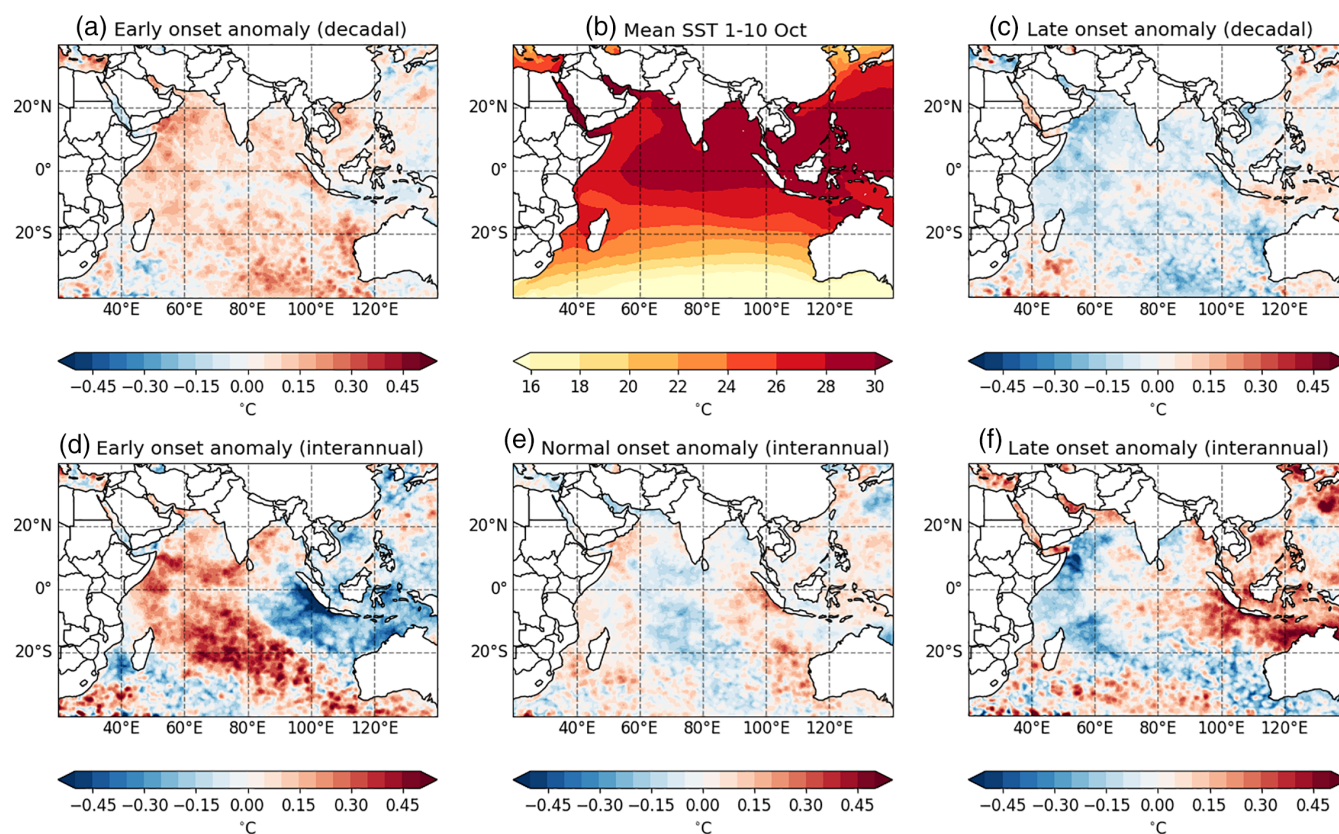


FIGURE 11 SST composites of decadal periods (top row) and interannual periods (bottom row) for (a) decadal early onset anomaly, (b) mean SST, (c) decadal late onset anomaly, (d) interannual early onset anomaly, (e) interannual normal onset anomaly, (f) interannual late onset anomaly

central Indian Ocean are generally warmer while the eastern part is cooler compared to the normal onset. In the late onset years the western Indian Ocean is cooler while the central and eastern Indian Ocean are warmer (Figure 11f). An analysis of the correlation of the filtered interannual variability of the onset and the dipole mode

index indicates negative statistically significant correlations (-0.51 , Figure S4). In previous studies enhanced total rainfall over the region has been linked to the positive phase of the Indian Ocean dipole (Black, 2005; Ummenhofer *et al.*, 2009; Hirons and Turner, 2018). In this study we have shown the link between the onset and

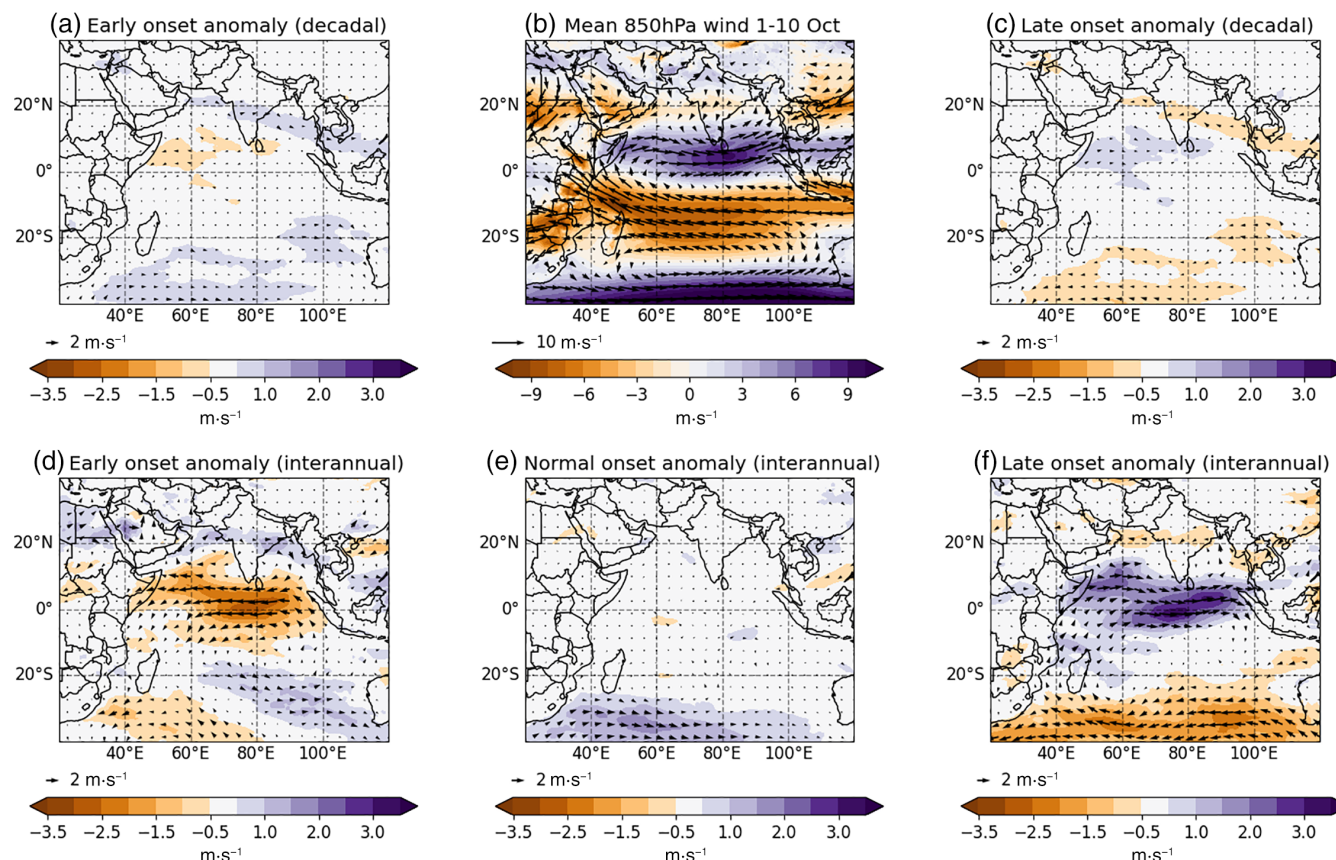


FIGURE 12 Mean flow (vectors) and zonal flow (shaded) composites of decadal periods (top row) and interannual periods (bottom row) for (a) decadal early onset anomaly, (b) mean circulation, (c) decadal late onset anomaly, (d) interannual early onset anomaly, (e) interannual normal onset anomaly, (f) interannual late onset anomaly

IOD, with positive (negative) phases linked to early (late) onset. While in the interannual case the anomalies show a dipole, the decadal case is dominated by a uniform temperature change across the basin. Comparing with the unfiltered composite analysis (Figure 7), it is clear that in the early onset years the decadal variability acts to increase the SSTs for the interannual timescale over western and central Indian Ocean.

3.6.2 | Circulation and zonal winds

The analysis for interannual and decadal variability is also conducted for the mean low-level flow and zonal winds (Figure 12). The mean flow is dominated by the southeasterly flow over the southern part of the Indian Ocean and the westerly flow dominates off the coast of Somalia (Figure 12b). On decadal timescales the anomalous easterlies (westerlies) for early (late) onset are weak and mostly close to zero (Figure 12a,c). For the interannual periods, early onset is associated with anomalous easterlies in the northern Indian Ocean (Figure 12d) and late onset is associated with anomalous westerlies

(Figure 12e). This indicates that at decadal timescale the influence of the zonal winds on the rainfall onset is very weak and that most of the signal from Figure 8 is due to variability on an interannual scale rather than on a decadal scale.

4 | CONCLUSIONS

In this study we have investigated the atmospheric and oceanic conditions that prevail prior to and during the short rains (OND) onset. The study showed that early onset is associated with enhanced rainfall over the region in October and November, however the relationship is weaker in December. On the other hand, late onset is associated with suppressed rainfall for all the months during the short rains season.

Composite analysis showed that early onset is linked to warmer SSTs over the western Indian Ocean, while there were no major differences in SST for the normal and late onset years over the western Indian Ocean. In early onset years there is an anomalous equatorial easterly moisture advection into Eastern Africa during the

first two dekads of October. Conversely, during the late onset years anomalous westerly flow is dominant and draws moisture out of the region. In dekad 1 of October early onset is linked to anomalous easterlies, while for the late onset years anomalous westerlies dominate the flow. This spatial pattern persists into dekad 2 and 3 of October; however, the magnitude of the anomalous easterly flow weakens.

In addition, we decompose the timeseries and analyse the interannual and decadal variability separately and its links with SSTs over the Indian Ocean basin. The analysis showed statistically significant correlations between the interannual variability of the onset and the dipole mode index. The analysis also showed that the variability in the onset is driven by both the interannual and decadal variability of the SSTs over the Indian Ocean. On decadal timescales, early onset years are linked with warm SSTs across the entire Indian Ocean basin, while on interannual timescales early onset is linked with warm SSTs in the western and central Indian Ocean and cool SSTs anomalies in the eastern Indian Ocean. In terms of winds, the anomalies are negligible for the decadal periods, with those associated with the interannual variability closely matching those found in the unfiltered analysis. These results warrant further work exploring the different drivers of onset variability on interannual and decadal timescales.

This study has developed an improved understanding of the relationship between the Indian Ocean SSTs and wind patterns and the variability in the onset of the Eastern Africa short rains season. Specifically, it has been shown that the state of the western Indian Ocean SSTs as early as the first dekad in September is associated with the nature of rainfall onset over Eastern Africa. This has immense implications for improving action-based forecasting. For example, knowing that there is an increased likelihood of early onset, and hence wetter Eastern Africa short rains, in early September significantly increases the lead time for effective preparedness action. However, these improvements in the understanding of drivers of onset variability will only be realized if they can be translated into reliable and timely forecasts products for the region. Further work on the representation of the atmospheric and oceanic drivers found in this study on the sub-seasonal to seasonal timescales can help understand the source of errors in the models and hence improve forecasts over the region.

ACKNOWLEDGEMENTS


This work was supported by UK Research and Innovation as part of the Global Challenges Research Fund, African SWIFT programme, grant number NE/P021077/1. Linda Hirons and Steve Woolnough were also supported by

National Centre of Atmospheric Science (NCAS) ACREW (Atmospheric hazard in developing Countries: Risk assessment and Early Warning). Analysis was conducted utilizing the Jasmin supercomputing system. We thank the U C Santa Barbara (CHIRPS; <https://www.chc.ucsb.edu/data/chirps>), Copernicus Data Store (ERA5; <https://cds.climate.copernicus.eu/>) and NOAA (SST; <https://www.ncdc.noaa.gov/oisst>) for provision of data.

AUTHOR CONTRIBUTIONS

Masilin Gudoshava: Conceptualization; formal analysis; investigation; methodology; visualization; writing – original draft. **Caroline Wainwright:** Conceptualization; formal analysis; investigation; methodology; visualization; writing – review and editing. **Linda Hirons:** Conceptualization; investigation; supervision; writing – review and editing. **Hussen S. Endris:** Resources; writing – review and editing. **Zewdu T. Segele:** Funding acquisition; supervision; writing – review and editing. **Steve Woolnough:** Conceptualization; funding acquisition; investigation; methodology; supervision; writing – review and editing. **Zachary Atheru:** Supervision; writing – review and editing. **Guleid Artan:** Funding acquisition; supervision.

ORCID

Masilin Gudoshava  <https://orcid.org/0000-0003-0315-9271>

REFERENCES

- Anyah, R.O. and Semazzi, F.H. (2007) Variability of East African rainfall based on multiyear RegCM3 simulations. *International Journal of Climatology*, 27(3), 357–371.
- Asnani, G.C. (1993) *Tropical Meteorology*. Poona: Indian Institute of Tropical Meteorology.
- Awange, J.L., Ogalo, L., Bae, K.H., Were, P., Omondi, P., Omute, P. and Omullo, M. (2008) Falling Lake Victoria water levels: Is climate a contributing factor? *Climatic Change*, 89(3), 281–297.
- Ayugi, B., Tan, G., Ullah, W., Boiyo, R. and Ongoma, V. (2019) Inter-comparison of remotely sensed precipitation datasets over Kenya during 1998–2016. *Atmospheric Research*, 225, 96–109.
- Bahaga, T.K., Fink, A.H. and Knippertz, P. (2019) Revisiting interannual to decadal teleconnections influencing seasonal rainfall in the Greater Horn of Africa during the 20th century. *International Journal of Climatology*, 39(5), 2765–2785.
- Banzon, V., Smith, T.M., Steele, M., Huang, B. and Zhang, H.M. (2020) Improved estimation of proxy sea surface temperature in the Arctic. *Journal of Atmospheric and Oceanic Technology*, 37(2), 341–349.
- Barrios, S., Bertinelli, L. and Strobl, E. (2010) Trends in rainfall and economic growth in Africa: a neglected cause of the African growth tragedy. *Review of Economics and Statistics*, 92(2), 350–366.
- Behera, S.K., Luo, J.J., Masson, S., Delecluse, P., Gualdi, S., Navarra, A. and Yamagata, T. (2005) Paramount impact of the

- Indian Ocean dipole on the East African short rains: a CGCM study. *Journal of Climate*, 18(21), 4514–4530.
- Beltrando, G. (1990) Space–time variability of rainfall in April and October–November over East Africa during the period 1932–1983. *International Journal of Climatology*, 10(7), 691–702.
- Beltrando, G. and Camberlin, P. (1993) Interannual variability of rainfall in the eastern Horn of Africa and indicators of atmospheric circulation. *International Journal of Climatology*, 13(5), 533–546.
- Black, E. (2005) The relationship between Indian Ocean sea-surface temperature and East African rainfall. *Philosophical Transactions of the Royal Society A: Mathematical, Physical and Engineering Sciences*, 363(1826), 43–47.
- Black, E., Slingo, J., and Sperber, K. R. (2003). An Observational Study of the Relationship between Excessively Strong Short Rains in Coastal East Africa and Indian Ocean SST. *Monthly Weather Review*, 131(1), 74–94. [https://doi.org/10.1175/1520-0493\(2003\)131<0074:aosotr>2.0.co;2](https://doi.org/10.1175/1520-0493(2003)131<0074:aosotr>2.0.co;2)
- Boos, W.R. and Emanuel, K.A. (2009) Annual intensification of the Somali jet in a quasi-equilibrium framework: observational composites. *Quarterly Journal of the Royal Meteorological Society*, 135(639), 319–335.
- Camberlin, P., Moron, V., Okoola, R., Philippon, N. and Gitau, W. (2009) Components of rainy seasons' variability in equatorial East Africa: onset, cessation, rainfall frequency and intensity. *Theoretical and Applied Climatology*, 98(3), 237–249.
- Camberlin, P. and Okoola, R.E. (2003) The onset and cessation of the “long rains” in Eastern Africa and their interannual variability. *Theoretical and Applied Climatology*, 75(1–2), 43–54.
- Damania, R., Desbureaux, S. and Zaveri, E. (2020) Does rainfall matter for economic growth? Evidence from global sub-national data (1990–2014). *Journal of Environmental Economics and Management*, 102, 102335.
- Dinku, T., Funk, C., Peterson, P., Maidment, R., Tadesse, T., Gadain, H. and Ceccato, P. (2018) Validation of the CHIRPS satellite rainfall estimates over Eastern Africa. *Quarterly Journal of the Royal Meteorological Society*, 144, 292–312.
- Dunning, C.M., Black, E. and Allan, R.P. (2018) Later wet seasons with more intense rainfall over Africa under future climate change. *Journal of Climate*, 31(23), 9719–9738.
- Dunning, C.M., Black, E.C. and Allan, R.P. (2016) The onset and cessation of seasonal rainfall over Africa. *Journal of Geophysical Research: Atmospheres*, 121(19), 11–405.
- Funk, C., Peterson, P., Landsfeld, M., Pedreros, D., Verdin, J., Shukla, S., Husak, G., Rowland, J., Harrison, L., Hoell, A. and Michaelsen, J. (2015) The climate hazards infrared precipitation with stations—a new environmental record for monitoring extremes. *Scientific Data*, 2(1), 1–21.
- Gudoshava, M., Misiani, H.O., Segele, Z.T., Jain, S., Ouma, J.O., Otieno, G., Anyah, R., Indasi, V.S., Endris, H.S., Osima, S. and Lennard, C. (2020) Projected effects of 1.5°C and 2°C global warming levels on the intra-seasonal rainfall characteristics over the Greater Horn of Africa. *Environmental Research Letters*, 15(3), 034037.
- Hersbach, H., Bell, B., Berrisford, P., Hirahara, S., Horányi, A., Muñoz-Sabater, J., Nicolas, J., Peubey, C., Radu, R., Schepers, D. and Simmons, A. (2020) The ERA5 global reanalysis. *Quarterly Journal of the Royal Meteorological Society*, 146(730), 1999–2049.
- Hirons, L. and Turner, A. (2018) The impact of Indian Ocean mean-state biases in climate models on the representation of the East African short rains. *Journal of Climate*, 31(16), 6611–6631.
- Indeje, M., Semazzi, F.H. and Ogallo, L.J. (2000) ENSO signals in East African rainfall seasons. *International Journal of Climatology*, 20(1), 19–46.
- Kijazi, A.L. and Reason, C.J.C. (2005) Relationships between intra-seasonal rainfall variability of coastal Tanzania and ENSO. *Theoretical and Applied Climatology*, 82(3), 153–176.
- Kimani, M.W., Hoedjes, J.C. and Su, Z. (2017) An assessment of satellite-derived rainfall products relative to ground observations over East Africa. *Remote Sensing*, 9(5), 430.
- Liu, W., Cook, K.H. and Vizzy, E.K. (2020) Influence of Indian Ocean SST regionality on the East African short rains. *Climate Dynamics*, 54(11), 4991–5011.
- MacLeod, D. (2018) Seasonal predictability of onset and cessation of the East African rains. *Weather and Climate Extremes*, 21, 27–35.
- Manatsa, D., Morioka, Y., Behera, S.K., Matarira, C.H. and Yamagata, T. (2014) Impact of Mascarene high variability on the East African “short rains”. *Climate Dynamics*, 42(5–6), 1259–1274.
- Marengo, J.A., Liebmann, B., Kousky, V.E., Filizola, N.P. and Wainer, I.C. (2001) Onset and end of the rainy season in the Brazilian Amazon Basin. *Journal of Climate*, 14(5), 833–852.
- Marteau, R., Moron, V. and Philippon, N. (2009) Spatial coherence of monsoon onset over western and central Sahel (1950–2000). *Journal of Climate*, 22(5), 1313–1324.
- Marteau, R., Sultan, B., Moron, V., Alhassane, A., Baron, C. and Traoré, S.B. (2011) The onset of the rainy season and farmers' sowing strategy for pearl millet cultivation in Southwest Niger. *Agricultural and Forest Meteorology*, 151(10), 1356–1369.
- Muglavai, E.M., Kipkorir, E.C., Raes, D. and Rao, M.S. (2008) Analysis of rainfall onset, cessation and length of growing season for western Kenya. *Agricultural and Forest Meteorology*, 148(6–7), 1123–1135.
- Mutai, C.C., Ward, M.N. and Colman, A.W. (1998) Towards the prediction of the East Africa short rains based on sea-surface temperature–atmosphere coupling. *International Journal of Climatology*, 18(9), 975–997.
- Nicholson, S.E. (2000) The nature of rainfall variability over Africa on time scales of decades to millenia. *Global and Planetary Change*, 26(1–3), 137–158.
- Nicholson, S.E. (2017) Climate and climatic variability of rainfall over Eastern Africa. *Reviews of Geophysics*, 55(3), 590–635.
- Nicholson, S.E. and Kim, J. (1997) The relationship of the El Niño–Southern oscillation to African rainfall. *International Journal of Climatology*, 17(2), 117–135.
- Odekunle, T.O. (2004) Rainfall and the length of the growing season in Nigeria. *International Journal of Climatology*, 24(4), 467–479.
- Ogallo, L.J. (1988) Relationships between seasonal rainfall in East Africa and the Southern Oscillation. *Journal of Climatology*, 8(1), 31–43.
- Ogallo, L.J. (1989) The spatial and temporal patterns of the East African seasonal rainfall derived from principal component analysis. *Journal of Climatology*, 9, 145–167.
- Ogallo, L.J. and Janowiak, J.E. (1988) Teleconnection between seasonal rainfall over East Africa and global sea surface

- temperature anomalies. *Journal of the Meteorological Society of Japan. Series II*, 66(6), 807–822.
- Okoola, R.E. (1999) A diagnostic study of the Eastern Africa monsoon circulation during the Northern Hemisphere spring season. *International Journal of Climatology*, 19(2), 143–168. [https://doi.org/10.1002/\(SICI\)1097-0088\(199902\)19:2<143::AID-JOC342>3.0.CO;2-U](https://doi.org/10.1002/(SICI)1097-0088(199902)19:2<143::AID-JOC342>3.0.CO;2-U).
- Omondi, P., Awange, J.L., Ogallo, L.A., Okoola, R.A. and Forootan, E. (2012) Decadal rainfall variability modes in observed rainfall records over East Africa and their relations to historical sea surface temperature changes. *Journal of Hydrology*, 464, 140–156.
- Omondi, P., Ogallo, L.A., Anyah, R., Muthama, J.M. and Ininda, J. (2013) Linkages between global sea surface temperatures and decadal rainfall variability over Eastern Africa region. *International Journal of Climatology*, 33(8), 2082–2104.
- Ongoma, V. and Chen, H. (2017) Temporal and spatial variability of temperature and precipitation over East Africa from 1951 to 2010. *Meteorology and Atmospheric Physics*, 129(2), 131–144.
- Owusu, A., Tesfamariam-Tekeste, Y., Ambani, M., Zebiak, S.E. and Thomson, M.C., 2017. *Climate Services for Resilient Development (CSR) Technical Exchange in Eastern Africa Workshop Report*. France: CGIAR, CGSpace.
- Philippon, N., Camberlin, P., Moron, V. and Boyard-Micheau, J. (2015) Anomalously wet and dry rainy seasons in equatorial East Africa and associated differences in intra-seasonal characteristics. *Climate Dynamics*, 45(7), 2101–2121.
- Recha, C.W., Makokha, G.L., Traore, P.S., Shisanya, C., Lodoun, T. and Sako, A. (2012) Determination of seasonal rainfall variability, onset and cessation in semi-arid Tharaka district, Kenya. *Theoretical and Applied Climatology*, 108(3), 479–494.
- Reynolds, R.W. (1993) Impact of Mount Pinatubo aerosols on satellite-derived sea surface temperatures. *Journal of Climate*, 6(4), 768–774.
- Riddle, E.E. and Cook, K.H. (2008) Abrupt rainfall transitions over the Greater Horn of Africa: observations and regional model simulations. *Journal of Geophysical Research: Atmospheres*, 113(D15).
- Saji, N.H., Goswami, B.N., Vinayachandran, P.N. and Yamagata, T. (1999) A dipole mode in the tropical Indian Ocean. *Nature*, 401(6751), 360–363.
- Schreck, C.J., III and Semazzi, F.H. (2004) Variability of the recent climate of Eastern Africa. *International Journal of Climatology*, 24(6), 681–701.
- Segele, Z.T. and Lamb, P.J. (2005) Characterization and variability of Kiremt rainy season over Ethiopia. *Meteorology and Atmospheric Physics*, 89(1–4), 153–180.
- Singh, P., Wani, S.P., Pathak, P., Sahrawat, K.L. and Singh, A.K. (2011) Increasing crop productivity and effective use of water in rainfed agriculture. In: *Integrated Watershed Management in Rainfed Agriculture*, pp. 315–347. London, UK: CRC Press (Taylor & Francis).
- Sivakumar, M.V.K. (1988) Predicting rainy season potential from the onset of rains in southern Sahelian and Sudanian climatic zones of West Africa. *Agricultural and Forest Meteorology*, 42(4), 295–305.
- Sohn, B.J. and Park, S.C. (2010) Strengthened tropical circulations in past three decades inferred from water vapor transport. *Journal of Geophysical Research: Atmospheres*, 115(D15).
- Sultan, B., Lejeune, Q., Menke, I., Maskell, G., Lee, K., Noblet, M., Sy, I. and Roudier, P. (2020) Current needs for climate services in West Africa: results from two stakeholder surveys. *Climate Services*, 18, 100166.
- Tierney, J.E., Smerdon, J.E., Anchukaitis, K.J. and Seager, R. (2013) Multidecadal variability in East African hydroclimate controlled by the Indian Ocean. *Nature*, 493(7432), 389–392.
- Ummenhofer, C.C., Sen Gupta, A., England, M.H. and Reason, C.J. (2009) Contributions of Indian Ocean sea surface temperatures to enhanced East African rainfall. *Journal of Climate*, 22(4), 993–1013.
- Wainwright, C.M., Marsham, J.H., Keane, R.J., Rowell, D.P., Finney, D.L., Black, E. and Allan, R.P. (2019) Eastern African Paradox rainfall decline due to shorter not less intense long rains. *npj Climate and Atmospheric Science*, 2(1), 1–9.

SUPPORTING INFORMATION

Additional supporting information may be found in the online version of the article at the publisher's website.

How to cite this article: Gudoshava, M., Wainwright, C., Hirons, L., Endris, H. S., Segele, Z. T., Woolnough, S., Atheru, Z., & Artan, G. (2022). Atmospheric and oceanic conditions associated with early and late onset for Eastern Africa short rains. *International Journal of Climatology*, 42(12), 6562–6578. <https://doi.org/10.1002/joc.7627>